PNNL-23411

Pacific Northwest
NATIONAL LABORATORY

Proudly Operated by Battelle Since 1965

Informal Preliminary Report on Comparisons of Prototype SPN-1 Radiometer to PARSL Measurements

June 2014

CN Long

U.S. DEPARTMENT OF
ENERGY

Prepared for the U.S. Department of Energy
under Contract DE-AC05-76RL01830

PACIFIC NORTHWEST NATIONAL LABORATORY
operated by
BATTELLE
for the
UNITED STATES DEPARTMENT OF ENERGY
under Contract DE-AC05-76RL01830

Printed in the United States of America

Available to DOE and DOE contractors from the
Office of Scientific and Technical Information,
P.O. Box 62, Oak Ridge, TN 37831-0062;
ph: (865) 576-8401
fax: (865) 576-5728
email: reports@adonis.osti.gov

Available to the public from the National Technical Information Service,
U.S. Department of Commerce, 5285 Port Royal Rd., Springfield, VA 22161
ph: (800) 553-6847
fax: (703) 605-6900
email: orders@ntis.fedworld.gov
online ordering: http://www.ntis.gov/ordering.htm

This document was printed on recycled paper.

(9/2003)

PNNL-23411

Informal Preliminary Report on Comparisons of Prototype SPN-1 Radiometer to PARSL Measurements

CN Long

June 2014

Prepared for the U.S. Department of Energy
under Contract DE-AC05-76RL01830

Pacific Northwest National Laboratory
Richland, Washington 99352

Informal Preliminary Report on Comparisons of Prototype SPN-1 Radiometer to PARSL Measurements

Dr. Charles N. Long
Atmospheric Radiation Measurement Program
Pacific Northwest National Laboratory
P. O. 999, MSIN: K9-24
Richland, WA, USA 99352
Ofc.: 1 (509) 372-4917
FAX: 1 (509) 372-6247
e-mail: chuck.long@pnl.gov

Introduction:

The prototype SPN-1 has been taking measurements for several months collocated with our PNNL Atmospheric Remote Sensing Laboratory (PARSL) solar tracker mounted instruments at the Pacific Northwest National Laboratory (PNNL) located in Richland, Washington, USA. The PARSL radiometers used in the following comparisons consist of an Eppley Normal Incident Pyrheliometer (NIP) and a shaded Eppley model 8-48 "Black and White" pyrgeometer (B&W) to measure the direct and diffuse shortwave irradiance (SW), respectively. These instruments were calibrated in mid-September by comparison to an absolute cavity radiometer directly traceable to the world standard group in Davos, Switzerland. The NIP calibration was determined by direct comparison, while the B&W was calibrated using the shade/unshade technique. All PARSL data prior to mid-September have been reprocessed using the new calibration factors. The PARSL data are logged as 1-minute averages from 1-second samples.

Data used in this report span the time period from June 22 through December 1, 2006. All data have been processed through the QCRad code (Long and Shi, 2006), which itself is a more elaborately developed methodology along the lines of that applied by the Baseline Surface Radiation Network (BSRN) Archive (Long and Dutton, 2004), for quality control. The SPN-1 data are the standard total and diffuse SW values obtained from the analog data port of the instrument. The comparisons use only times when both the PARSL and SPN-1 data passed all QC testing. The data were further processed and analyzed by application of the SW Flux Analysis methodology (Long and Ackerman, 2000; Long and Gaustad, 2004, Long et al., 2006) to detect periods of clear skies, calculate continuous estimates of clear-sky SW irradiance and the effect of clouds on the downwelling SW, and estimate fractional sky cover.

Aggregate Measurement Comparisons:

Figure 1 shows a comparison of 15-minute averages of the total SW, both measured (blue) and estimated clear-sky. 15-minute averages are used to minimize the effects of small timing differences, and radiometer sampling differences, between the two radiometer systems. As this plot shows, an RMS line fitted through the measured data (black line) shows the SPN-1 reads lower than the PARSL sum of the direct plus diffuse SW. For a PARSL value of 900 Wm^{-2}, the SPN-1 gives about 850 Wm^{-2}. This same offset is naturally also present in the clear-sky estimates, since these estimates are derived from detected clear-sky data for each system.

Figure 2 shows the comparison of the diffuse SW measurements and clear-sky estimates, similar to Figure 1. Again, the SPN-1 diffuse is less than the corresponding PARSL values, but in the diffuse case the slope of the RMS line fitted to the measured data is even greater than that for the total SW in Figure 1.

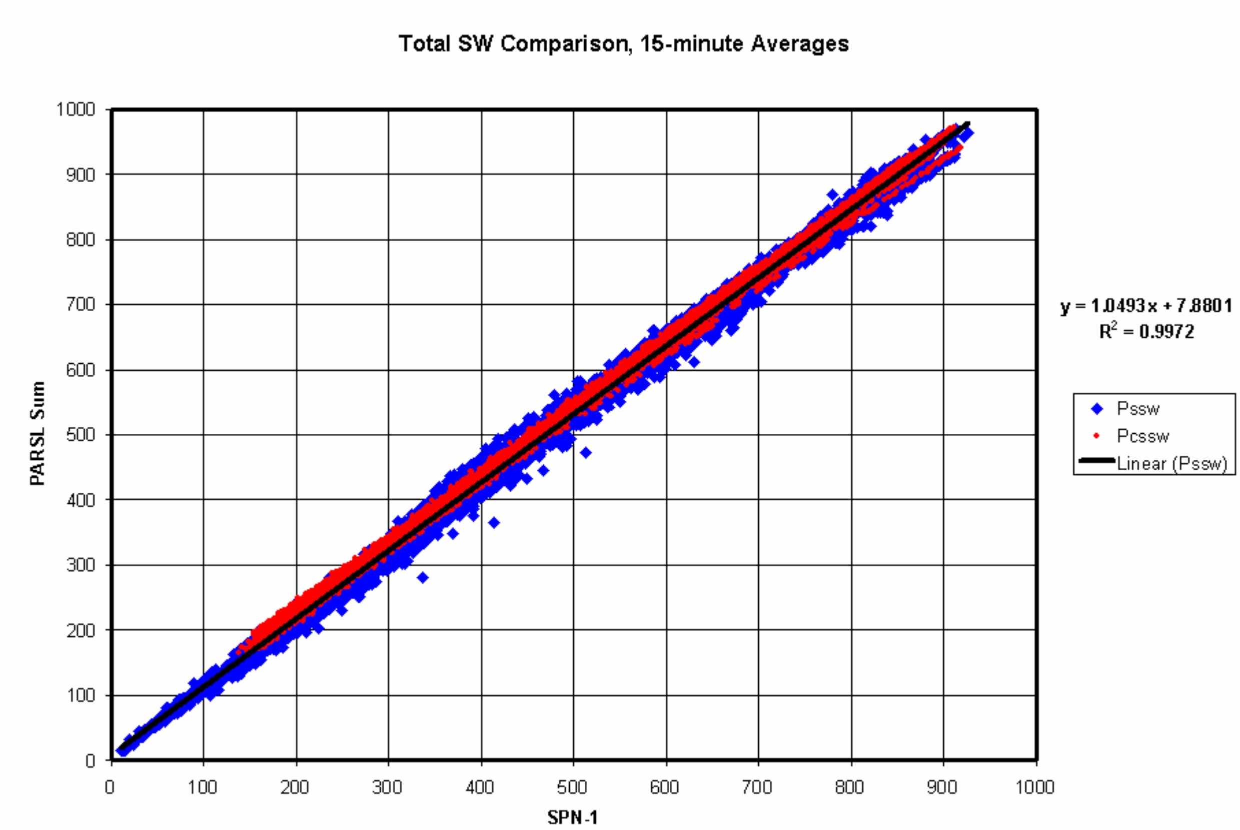

Figure 1: Comparison of PARSL and SPN-1 measured (blue) and clear-sky (red) total SW.

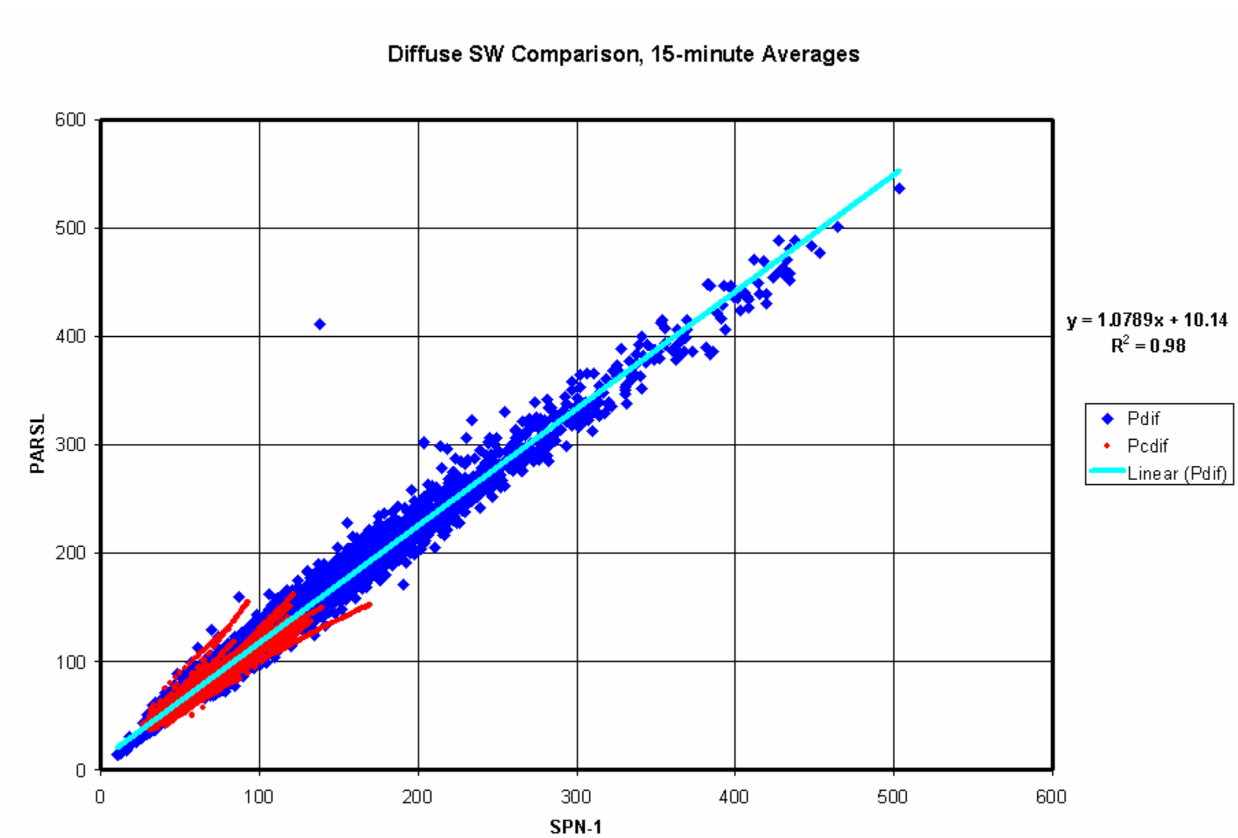

Figure 2: Comparison of PARSL and SPN-1 measured (blue) and clear-sky (red) diffuse SW.

In addition, there are larger excursions from agreement for the estimated clear-sky diffuse SW. This latter phenomenon will be addressed later in this report.

These two plots suggest that the calibration of the SPN-1 is a bit off, such that all irradiance values are underestimated. Figure 3 shows a comparison for total SW similar to Figure 1, but in this case the RMS fitted line is forced through zero. Thus the slope can be used as an “adjustment factor” to normalize the SPN-1 total SW data to the PARSL data. This slope suggests that the SPN-1 total SW needs to be increased on average by about 6% to match that from the PARSL sum of direct plus diffuse SW. Multiplying the SPN-1 total SW by a factor of 1.06 does indeed produce better agreement (not shown), but multiplying the SPN-1 diffuse SW by a factor of 1.06 still results in the SPN-1 data being less than the PARSL shaded B&W data by about 8% as shown in Figure 4. Figure 5 shows the PARSL minus SPN-1 adjusted diffuse SW difference plotted versus fractional sky cover as estimated by the Flux Analysis methodology (Long et al., 2006) applied to the PARSL data, as well as the fractional difference calculated as the difference divided by the PARSL diffuse SW. RMS lines fitted through the data indicate no significant relationship to fractional sky cover, suggesting that the low diffuse SW bias of the SPN-1 is not to first order related to any spectral response function of the SPN-1. This result is expected given the fairly flat spectral response function illustrated in the lower left plot on page 2 of the SPN-1 datasheet v2, Nov 06 provided by the manufacturer.

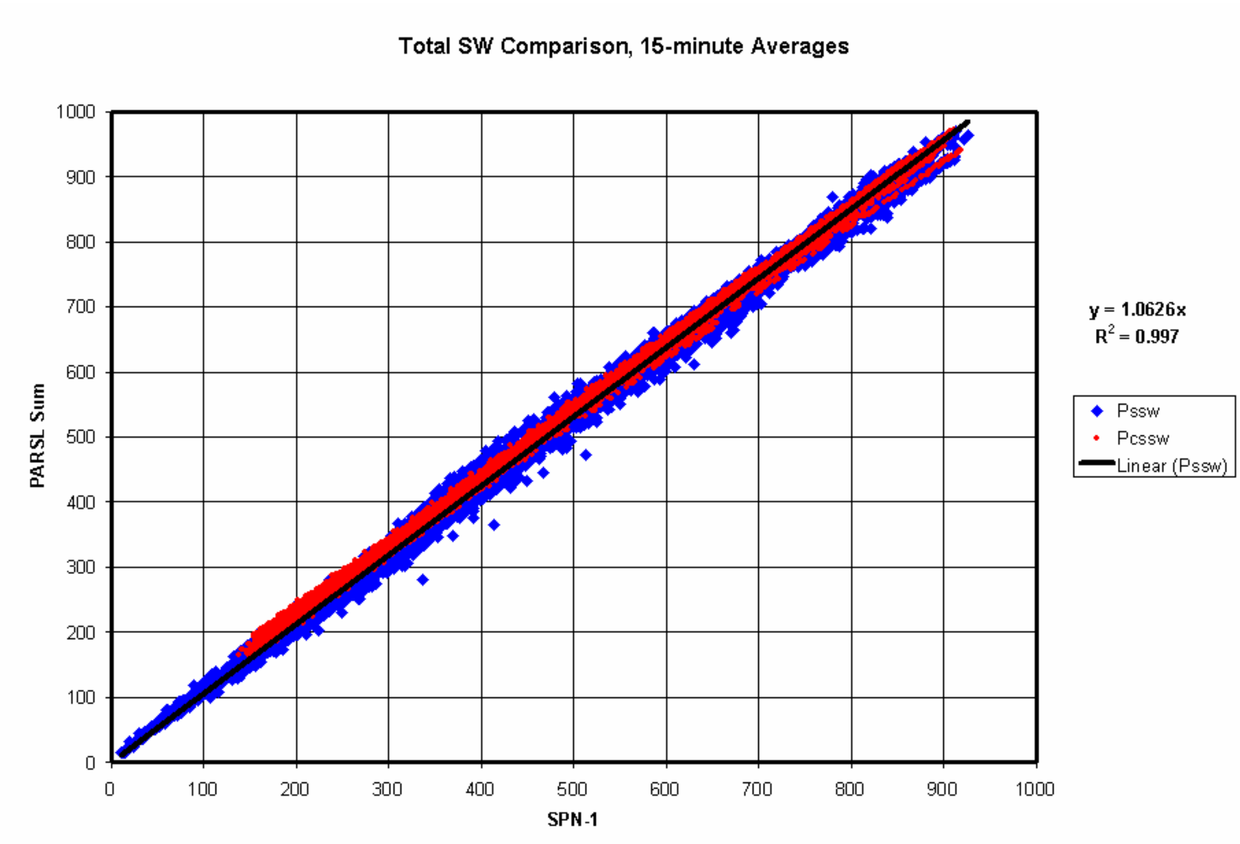

Figure 3: Similar to Figure 1, but with RMS fitted line forced through zero.

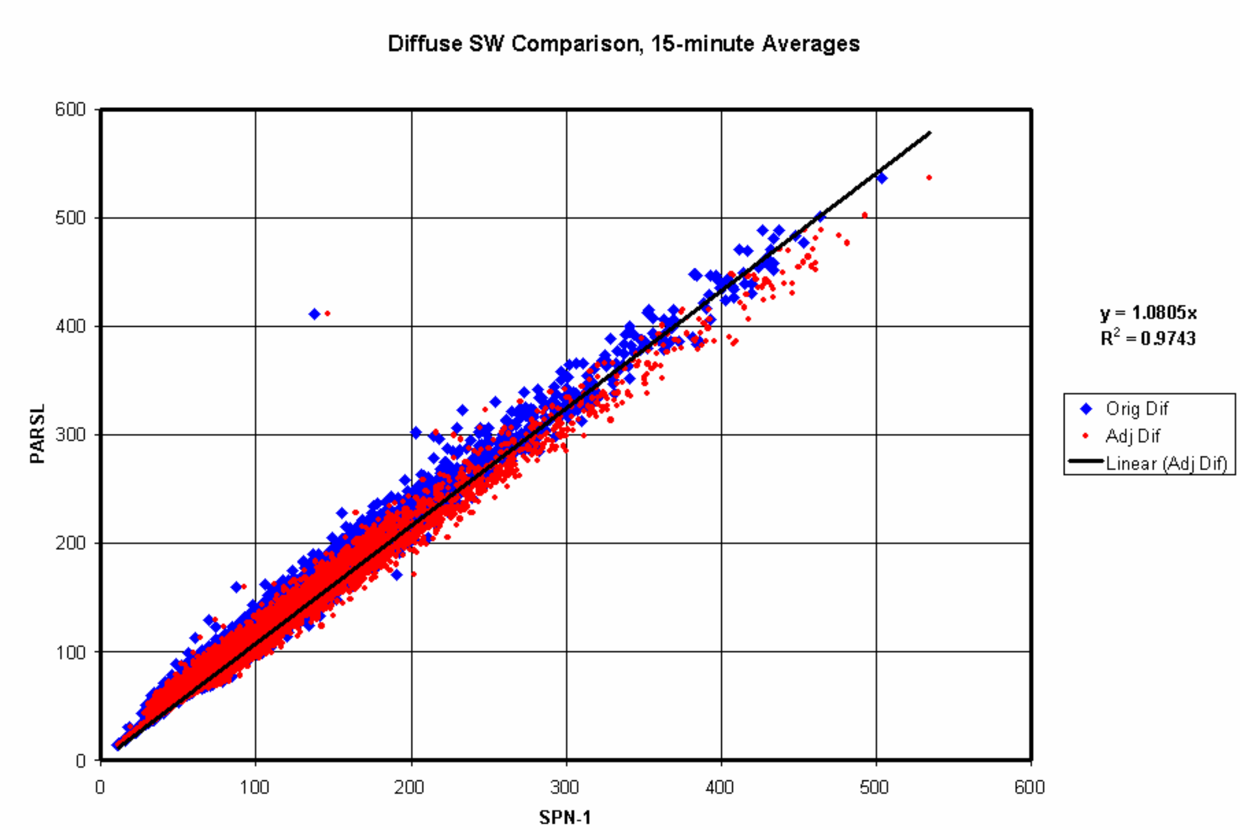

Figure 4: Similar to Figure 2, but with RMS line fitted to the adjusted diffuse data and forced through zero.

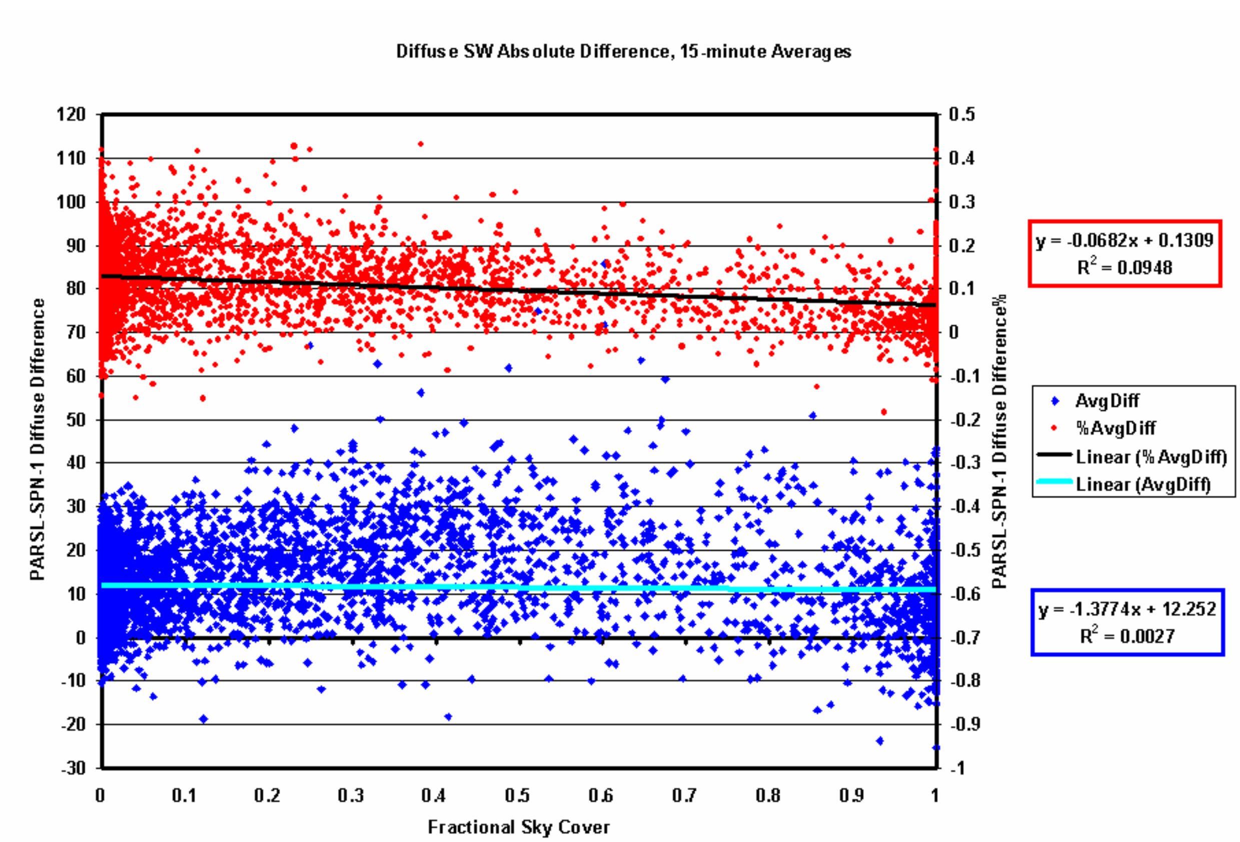

Figure 5: PARSL minus SPN-1 diffuse SW difference versus fractional sky cover.

Having the SPN-1 diffuse SW proportionally lower than the SPN-1 total SW naturally affects the ratio of diffuse over total SW, hereafter called the "diffuse ratio". Figure 6 shows the comparison of diffuse ratio between the SPN-1 and PARSL data. As expected, the SPN-1 diffuse ratio is less than the corresponding PARSL ratio. However, this difference manifests itself more as a constant offset rather than a multiplicative phenomenon, as evidenced by the RMS line fitted to the data. The slope of the fitted line is very nearly unity, with a constant offset of about 2-3%. This result, as also alluded to in Figure 4, suggests that the additional diffuse differences (above that for the total SW) is also effectively multiplicative in nature. This is good news because, as will be shown, the SPN-1 data as is can still be used to good extent in the SW Flux Analysis methodology, which is my primary goal.

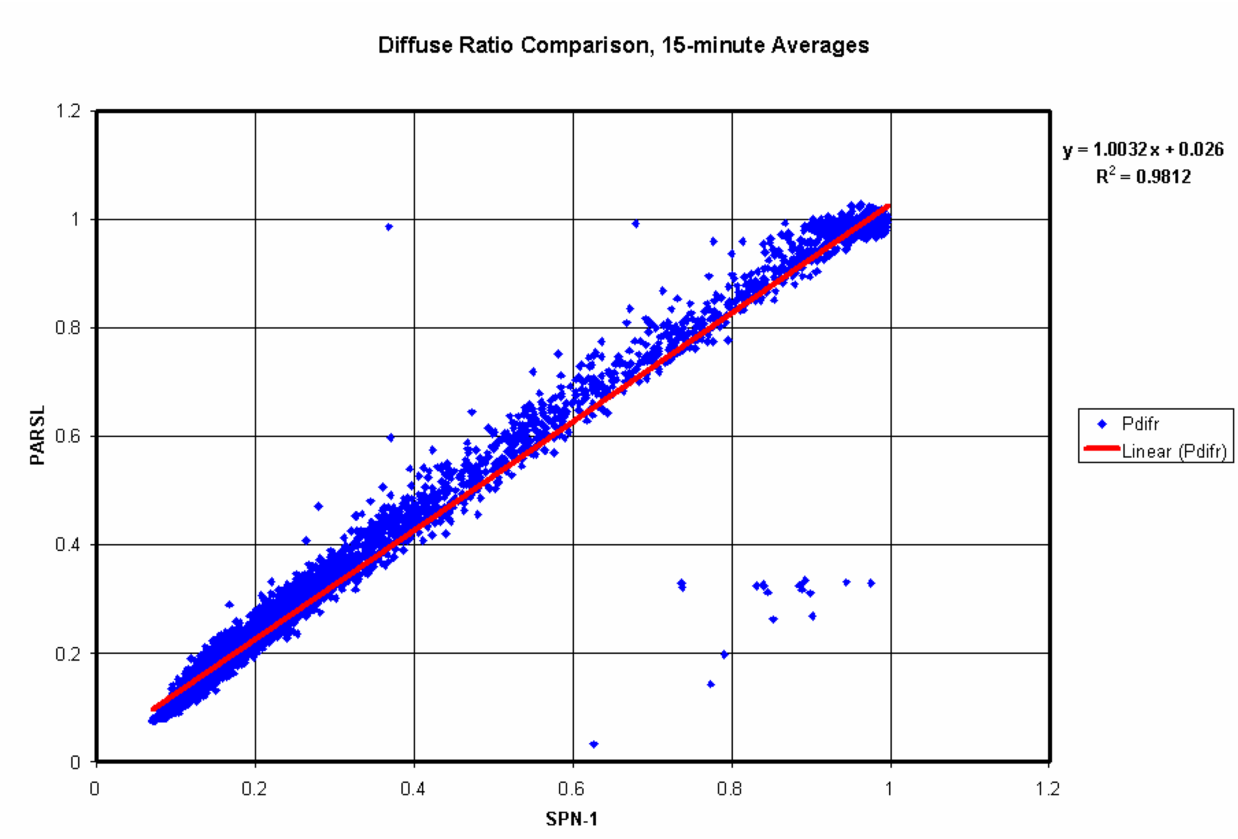

Figure 6: Comparison of PARSL and SPN-1 diffuse ratio, and RMS fitted line.

Use of SPN-1 Data for the SW Flux Analysis Methodology:

As described in Long and Ackerman (2000), analysis of the time series of total and diffuse SW measurements can be used to detect periods of clear-sky occurrence. If "enough" clear sky data on a given day spanning a sufficient relative range of solar zenith angle is detected, then the clear-sky data can be used to fit empirical functions that represent the clear-sky total SW and diffuse ratio for that day. The fit coefficients are interpolated for cloudy periods, and thus continuous estimates of clear-sky total, diffuse, and direct SW can be calculated. These clear-sky values are then used to estimate the effect of clouds on the downwelling irradiances, and to estimate the fractional sky cover present (Long et al., 2006). The basic measurements needed are those of total and diffuse SW, at a time resolution sufficient for monitoring the variability through time over an 11 to 21 minute time span. Thus while the BSRN recommended 1-minute data resolution is best, it has been shown that up to 5-minute data can work, though with somewhat degraded performance. It is important to note that since clear-sky measurements are used for fitting the clear-sky functions, the clear-sky estimates themselves exhibit the same instrument characteristics such as cosine response, calibration drift through time, etc. as the instruments themselves. While this could be considered a negative in that the clear-sky estimates naturally can be of no greater accuracy than the measurements, when using the clear-sky values relative to the measurements the instrument characteristics tend to have significantly less influence. For example, since the total SW is basically a calibration factor times the voltage signal from a thermopile detector, the ratio of measured over clear-sky total SW effectively cancels out the calibration constant and becomes a ratio of measured over clear-sky voltages. Thus in this case calibration errors and drifts, as well as cosine response characteristics, are largely removed from the resultant "effective cloud transmissivity" value.

The SW Flux Analysis methodology uses four basic tests to determine whether a given datum represents clear-sky or not. Two tests look at the magnitude of the total and diffuse SW, respectively. One test compares the change over a short time of the total SW to the corresponding change in top-of-atmosphere SW. The most sensitive test looks at the standard deviation of the diffuse ratio, normalized to remove solar zenith angle dependence, over an 11-minute span. Thus in order for the total and diffuse SW measurements to be useful, they must be nominally somewhere within the realm of the actual SW irradiance values, and not exhibit significant “noise” characteristics in the time series. As will be shown, the SPN-1 does well on the magnitude issue, but does not do as well on the time series “noise” issue.

Figure 7 shows the daylight time series of total and diffuse SW from both the SPN-1 and PARSL for July 8, 2006. For this plot, the SPN-1 data have not been adjusted by the normalization factor described previously, thus both the total and diffuse SW are less than the corresponding PARSL values. This was a clear day throughout the daylight period, though some thin haze occurred near local noon as evidenced by the variability in the PARSL total SW time series. Note in this plot that the SPN-1 time series exhibits more variability than the corresponding PARSL measurements, especially for the diffuse SW.

Figure 8 focuses on the diffuse time series only, and includes the SPN-1 "adjusted" diffuse as well as a calculated diffuse that would be produced by Rayleigh (molecular) scattering alone for a surface pressure of 1000 mb. The SPN-1 adjusted diffuse does show better average agreement with the PARSL data between roughly 0830 to 1530 LST, but the entire time series is anomalously noisy for clear-sky measurements. Additionally, both the raw and adjusted SPN-1 data from about 0430 to 0600 are less than the corresponding Rayleigh diffuse irradiance, a physical impossibility. This "sub-Rayleigh" behavior occurs at different times throughout the 6 months of the study period under dry, low haze clear-sky conditions.

Having the SPN-1 diffuse SW proportionally less than the total SW produces a lower diffuse ratio than that for the PARSL measurements (Figure 9) in the early part of the morning and late afternoon. The diffuse ratio is also naturally more "noisy" that the PARSL time series. This noisy characteristic is even more evident in the normalized diffuse ratio time series, shown in Figure 10, which is used in one of the tests for clear-sky. (See Long and Ackerman, 2000 for a detailed description of the normalized diffuse ratio.) Because of this increased noise on an obviously very clear day, the detection of clear-sky data suffers for the SPN-1 data. Figure 11 shows the number of detected clear-sky data each day of the study period for both the SPN-1 and PARSL measurements. As this plot shows, the SPN-1 data analysis consistently detected less clear-sky data than the PARSL analysis as a result of the ":noisy" behavior. One result is the differences in agreement for clear-sky diffuse SW shown in Figure 2, where some days were fitted for the PARSL data but had interpolated coefficients for the SPN-1 because there were too few detected clear-sky SPN-1 data for fitting. For both these analyses the normalized diffuse ratio standard deviation limit was set to the standard value of 0.0012 (See Long and Gaustad, 2004). As noted in Long and Ackerman (2000) this standard deviation limit can be set to a higher value to help compensate for noisy systems, but the trade-off is then less sensitivity to thin cloud or small cloud fraction occurrence. Given the results here, it would likely be useful to set the standard deviation limit for the SPN-1 to a higher value in order to detect more of the clear-sky data.

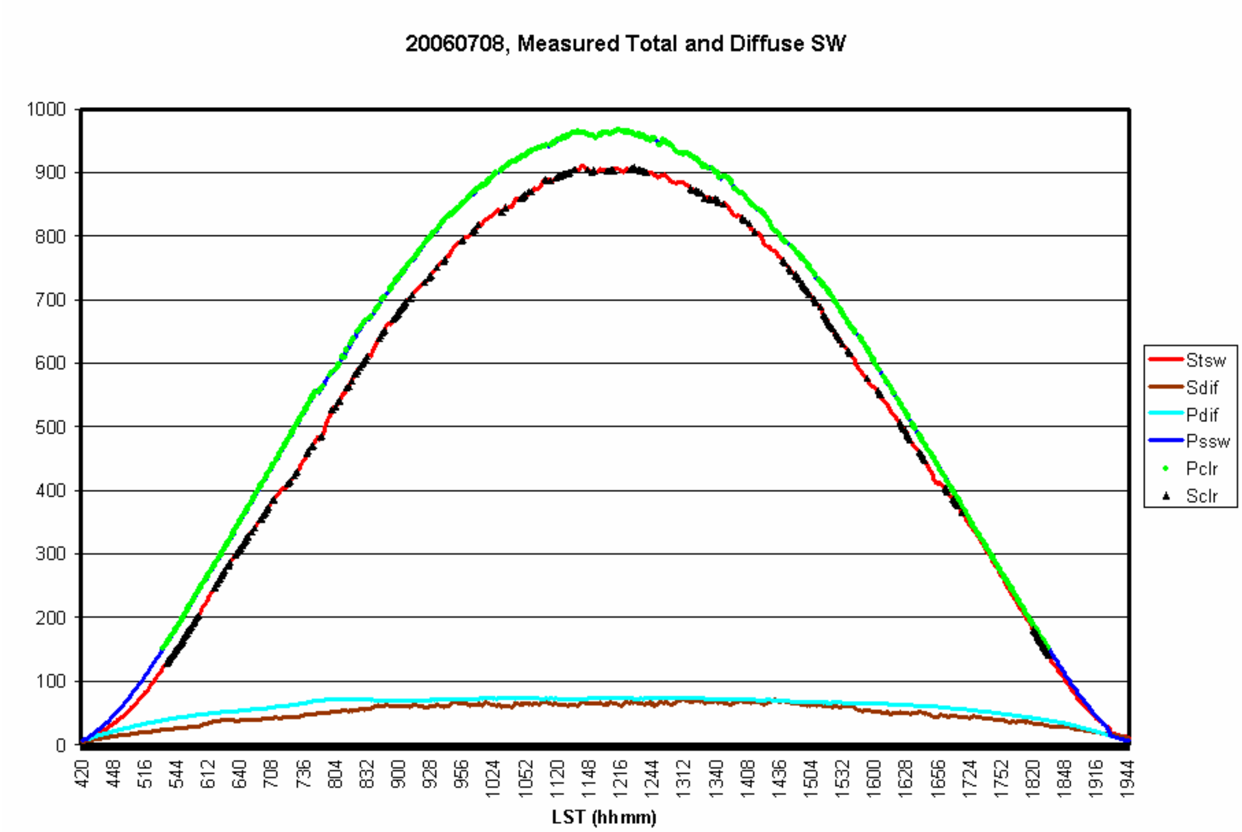

Figure 7: Time series of daylight PARSL and SPN-1 total and diffuse SW for July 8, 2006. Green and black dots denote data that were labeled as clear-sky by the SW Flux Analysis.

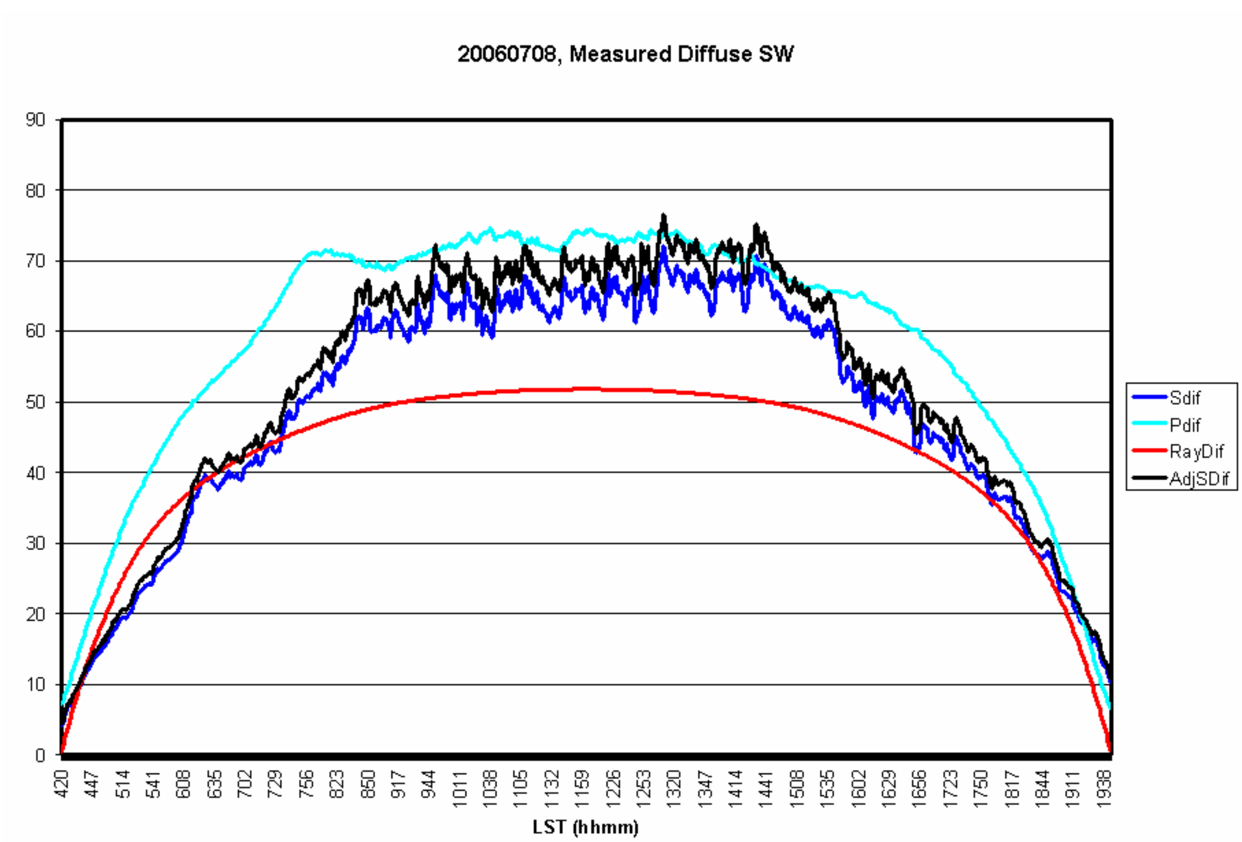

Figure 8: Time series of daylight PARSL and SPN-1 diffuse SW for July 8, 2006.

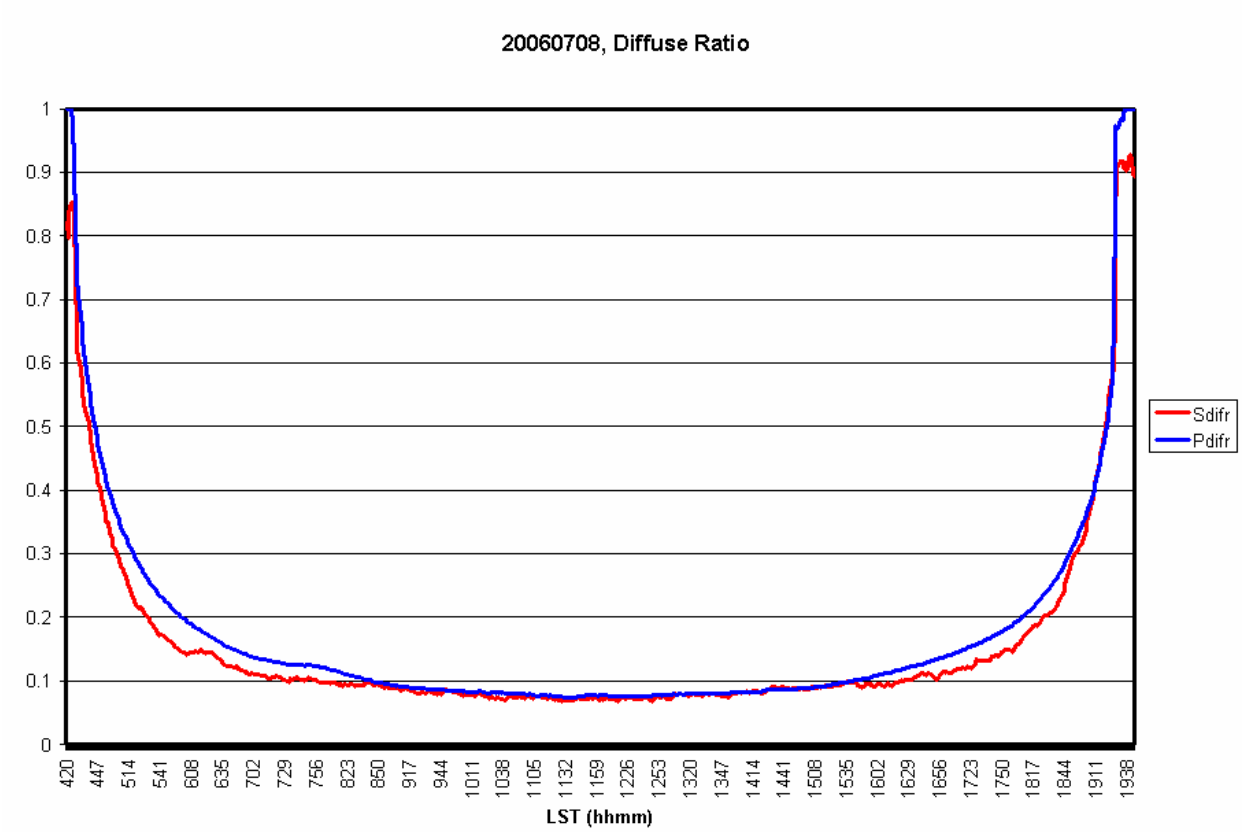

Figure 9: Time series of daylight PARSL and SPN-1 diffuse ratio for July 8, 2006.

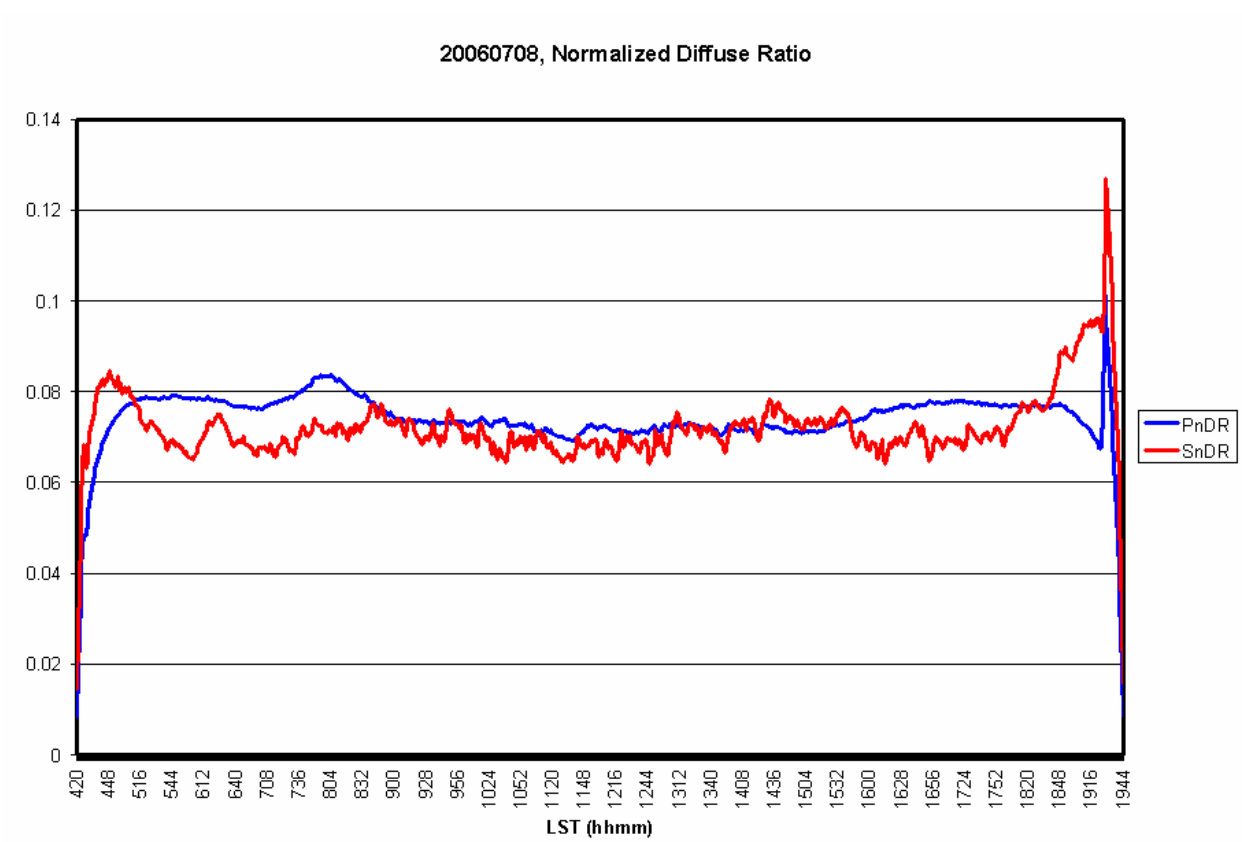

Figure 10: Time series of daylight PARSL and SPN-1 normalized diffuse ratio for July 8, 2006.

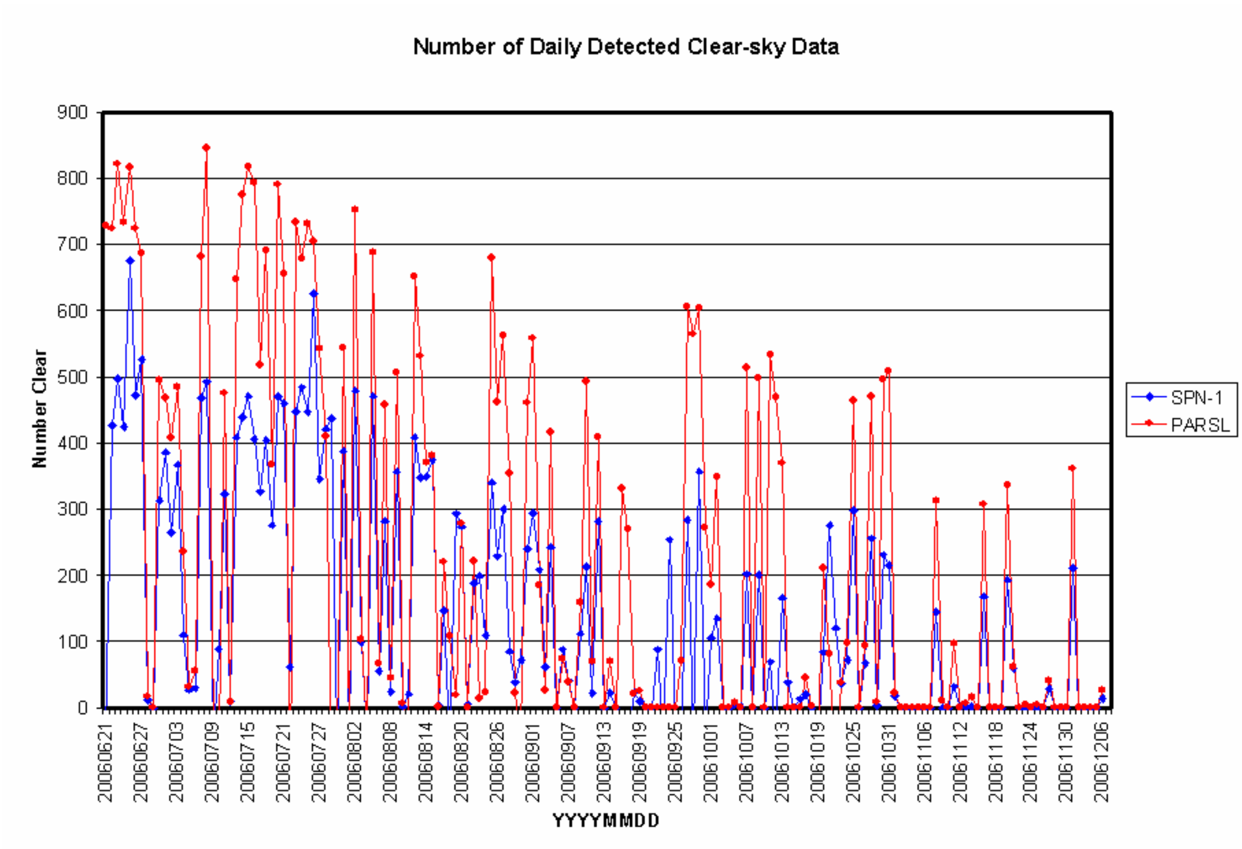

Figure 11: Number of detected clear-sky data per day for PARSL and SPN-1 data.

Investigation of several clear-sky days suggests a value of 0.002 might be nominal, though again making the methodology less sensitive to thin cloud or small cloud presence.

To investigate the SPN-1 diffuse SW low bias and noise issues, 5-second samples of the seven separate channels were logged starting August 14, 2006. Figure 12 shows comparisons similar to those in Figures 7-10, but for the clear-sky day of August 25, 2006. For this day, the adjusted SPN-1 diffuse SW is again consistently less than the PARSL diffuse. While the PARSL diffuse time series exhibits greater variability than was evident on July 8, the SPN-1 time series is once again far noisier. Figure 13 shows the separate raw SPN-1 channel values for this day, with the Y-axis range limited to a maximum value of 40 to focus on the minimum channel values used to calculate the diffuse SW. This plot illustrates that while some of the larger excursions occur in the transition from one channel to another being the lowest readings; by far most of the noise characteristics are inherent in the channel values themselves. Comparing Figure 13 to Figure 12 (upper right) shows that there are actually two levels of "noise" present. The first is related to the samples themselves. But the data in Figure 12 are 1-minute averages of (so I understand) 2-second samples, thus much of the small scale random noise is averaged out. But as Figure 13 shows, for periods of time on the order of hourly the same detector is consistently the minimum value. And these 1-minute averages still exhibit a drifting about in magnitude that is not inherent in the clear-sky diffuse SW for this clear-sky day, nor for the clear-sky day of July 8 (Figure 9), as shown by the PARSL diffuse SW measurements on these days. Thus transitioning from channel to channel is not the cause of the SPN-1 anomalous diffuse noise problem, there is some other cause inherent in each channel itself.

Examination of Figure 13 also reveals that the oscillation of the noise pattern is correlated across the channels, i.e. when the minimum channel increases or decreases so do the other channels. One rather unique feature of the SPN-1 design in the inclusion of internal heaters to mitigate the formation of dew and frost on the radiometer dome. These heaters are located internally for the SPN-1, beneath the mounting plate of the detector diffusers. As noted before, the data collected at PNNL shows occurrences of sub-Rayleigh diffuse SW measurements, often occurring in the early morning as is the case in Figure 8. Our temperature

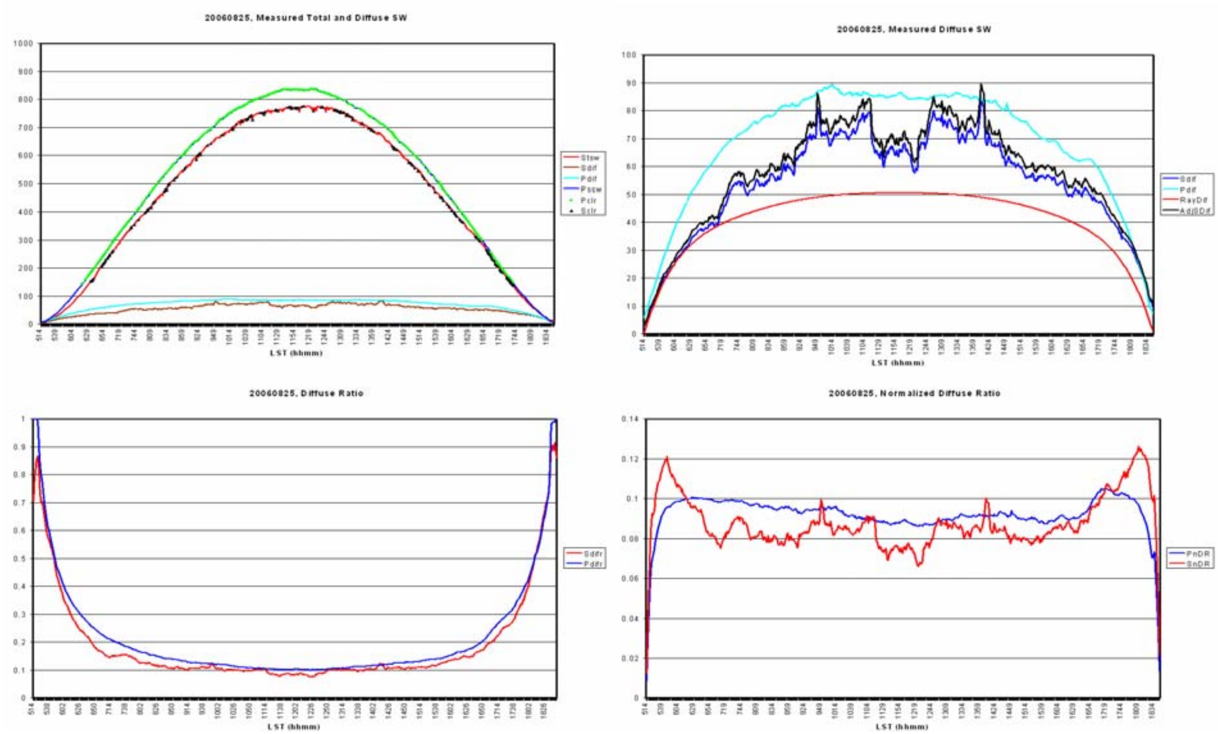

Figure 12: Time series similar to Figs 7-10, but for August 25, 2006.

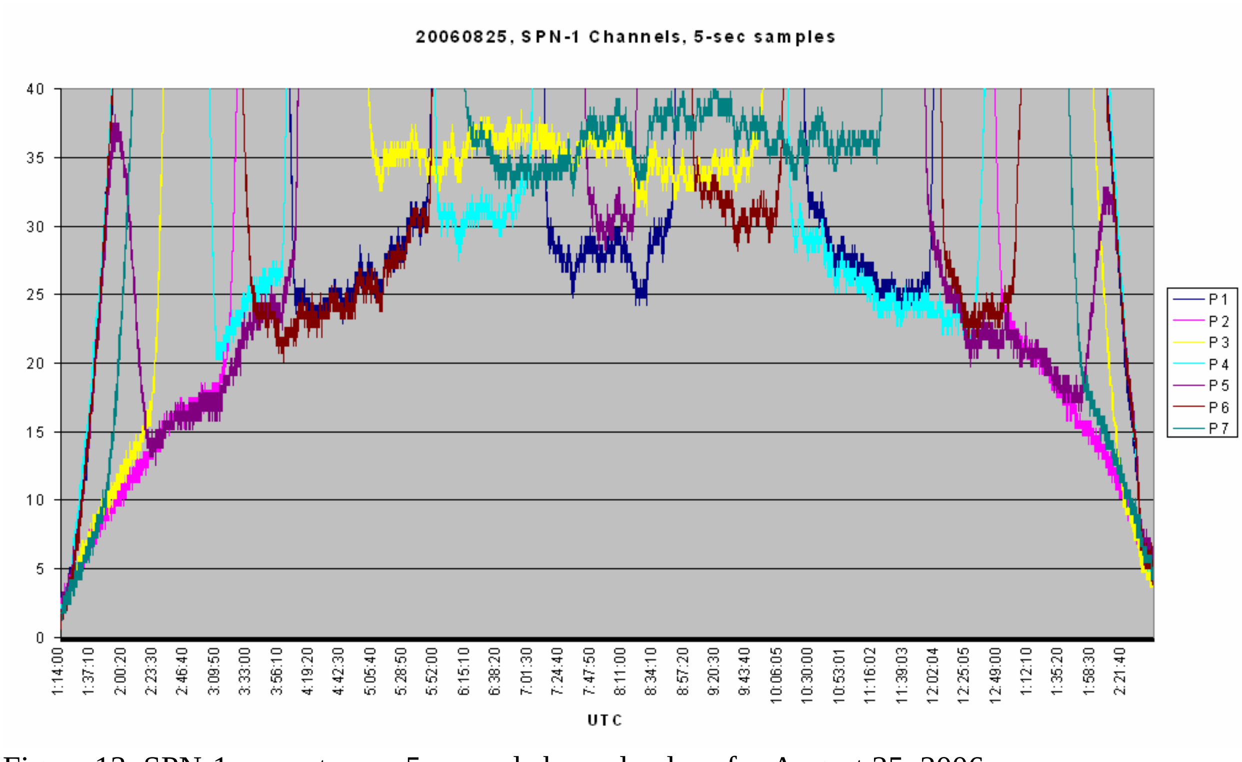

Figure 13: SPN-1 separate raw 5-second channel values for August 25, 2006.

measurements show that early mornings on clear-sky days feature a more pronounced warming from the lower night time temperatures caused by radiational cooling. Thus at these times it is more likely that the SPN-1 heaters are steadily on. For warmer ambient temperatures, one suspects that the heaters are switching on and off, or from lower to higher power. The correlation of noise oscillation across all the channels, along with the sub-Rayleigh measurements, suggests that the SPN-1 thermopile detectors might be seeing the influence of the heaters as interference with the heat transfer from the hot to cold junctions. In standard, non-heated single black thermopile detector pyranometers such as the Eppley model PSP, the interference with the heat flow has been described as a "thermal offset" or "IR loss" (Dutton et al., 2000; Younkin and Long, 2004) represented as a reverse heat flow through the thermopile. Night time negative offset data are used to detect this IR loss problem, and used to develop relationships to collocated pyrgeometer detector and case and dome temperature data in order to apply a correction. However the SPN-1 data are limited to a lowest value of zero by the on-board processing, thus no negative signal output is available to test for the presence of negative night time values. In order to further investigate the possibility of heater influence, the ability to “turn off” the heaters is needed as a minimum. Output of the internal temperature sensor and logging of sub-zero values would also be of particular use.

The above noted comparative bias and variability of the SPN-1 diffuse SW measurements adversely affects usefulness of the current data as absolute measures of diffuse irradiances. However the retrieved parameters from the SW Flux Analysis methodology are calculated from relative differences and ratios which, as pointed out previously, have a decreased sensitivity to biases and multiplicative offsets. This decreased sensitivity is shown in Figure 14 which compares the effective cloud transmissivity (calculated as a ratio of the measured over clear-sky total SW) retrieved for both the PARSL sum (blue) and unshaded pyranometer (red) total SW to that derived from the raw (i.e. unadjusted) SPN-1 total SW measurements. Despite the roughly 6% difference between the SPN-1 total SW and the PARSL sum SW shown in Figure 3, the comparison in Figure 14 exhibits no significant bias or offset between the three retrievals. The same is true for the SW cloud effect, calculated as the measured minus the clear-sky total SW such that a negative number relates to clouds decreasing the downwelling SW reaching the surface, as shown in Figure 15.

The cloud effective transmissivity and cloud effect calculations involve only the total SW measurements. The estimation of fractional sky cover (Long et al., 2006), however, additionally involves the diffuse SW. Here again, even the noted low bias of the SPN-1 diffuse measurements does not introduce a multiplicative bias in the retrieved sky cover comparison shown in Figure 16, as evidenced by a fitted line slope of nearly 1 and virtually no significant offset. The increased scatter about the fitted line is the result of the noted SPN-1 diffuse SW noisiness, as well as the difference in days that were fitted discussed previously (Figures 2 and 11). The standard deviation from the fitted line of about 0.06 given in Table 1 is roughly twice that shown previously for comparisons between tracker-mounted systems and standard unshaded pyranometers (Long et al., 2006).

Table 1 summarizes some statistics of the various comparisons presented in this study. For these statistics the “Medfit” routine from Numerical Recipies (Press et al., 1986) was used for line fitting. The Medfit routine minimizes the absolute deviations, thus eliminating outliers from the fitting. In this way, some of the scatter caused by anomalies such as birds or insects interfering with one of the measurements is eliminated and the prevalent relationships are fitted. Thus these slopes and offsets differ somewhat from those included in the previous figures which were derived using sum-of-least-squares fitting for all the data. The standard deviations then are calculated with respect to the fitted line.

In both the SPN-1 total and diffuse SW cases, applying an adjustment factor of 1.06 moved the slope of the fitted lines closer to unity, but had no influence on either the offsets or the standard deviation from the fitted lines. The resultant standard deviations for these 15-minute average data are about 10 Wm^{-2} and 14 Wm^{-2} for the total and diffuse SW, respectively. For the diffuse ratio, as noted previously the slope is very near unity,

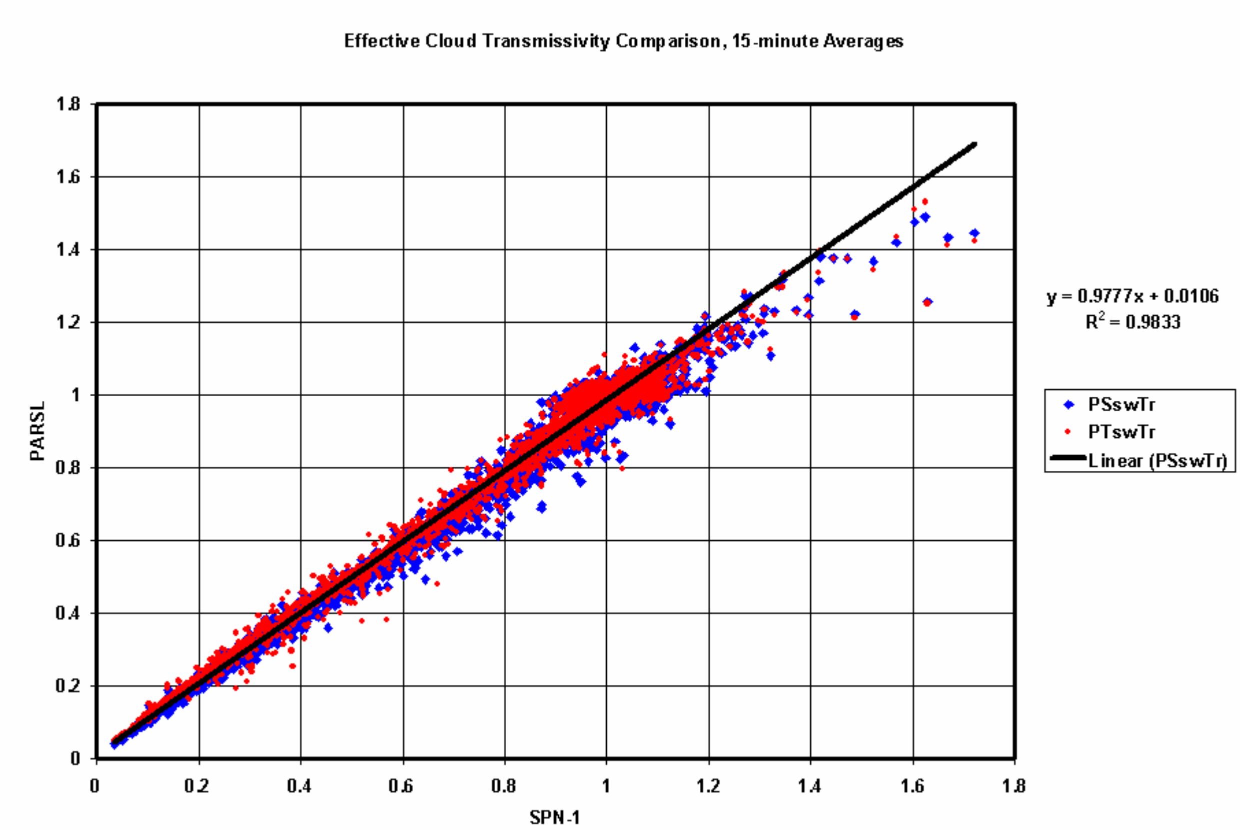

<u>Figure 14:</u> Comparison of PARSL and SPN-1 effective cloud transmissivity retrievals.

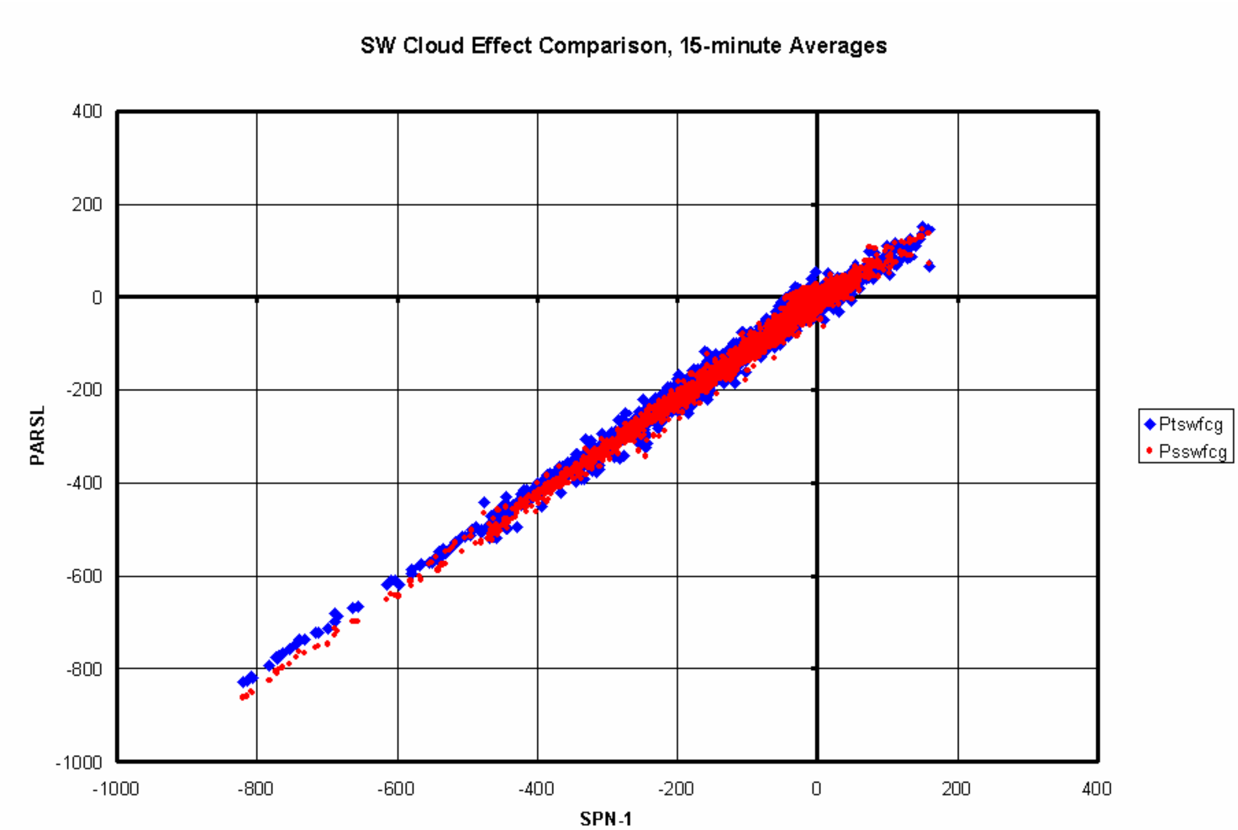

<u>Figure 15:</u> Comparison of PARSL and SPN-1 SW cloud effect for both the PARSL sum and unshaded pyranometer data.

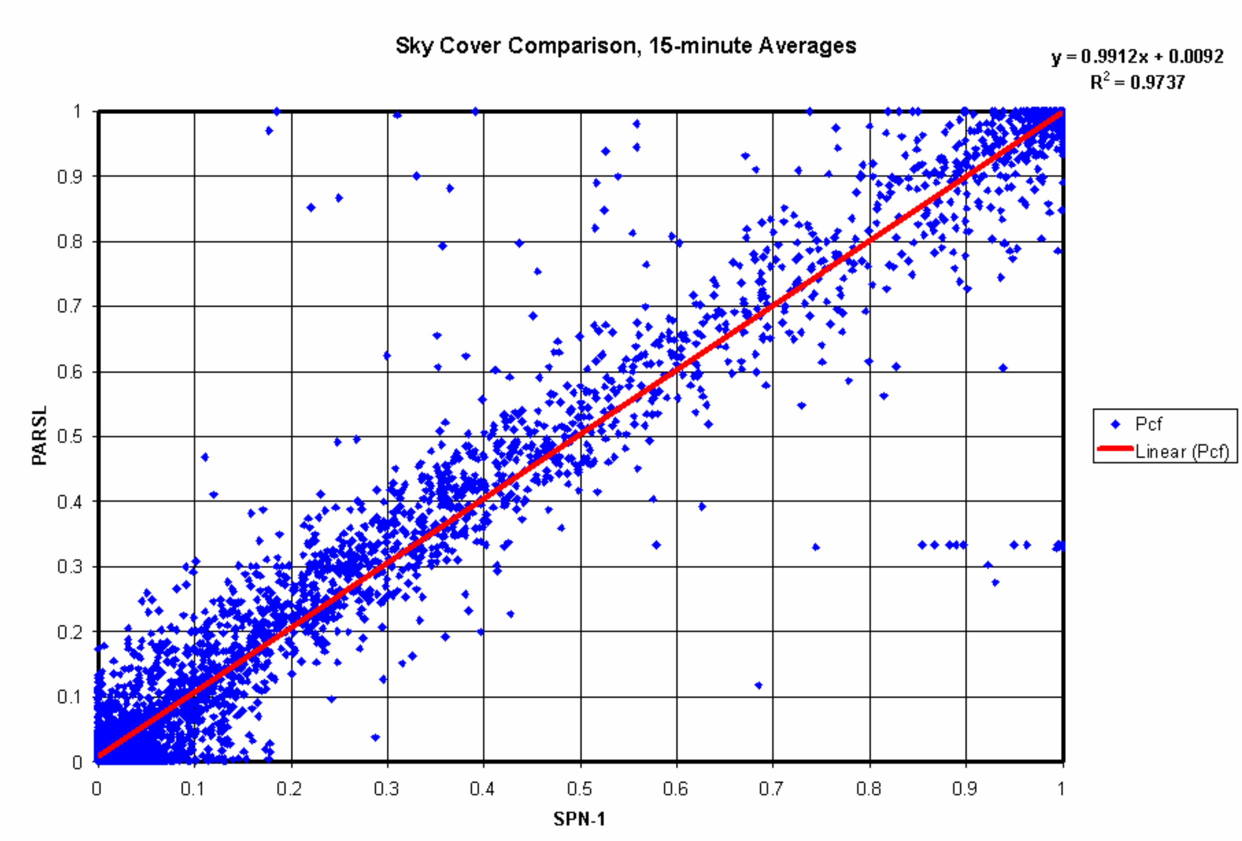

Figure 16: Comparison of PARSL and SPN-1 SW fractional sky cover retrievals.

Table 1: Summary of slopes and offsets of fitted lines, as well as the standard deviations from the fitted line, for the comparisons presented in this study

Comparison	Slope	Offset	StDev
STsw-PSsw	1.0493	7.9	13.6
SAdjTsw-PSsw	0.9875	7.9	13.6
Sdif-Pdif	1.0789	10.1	10.2
SAdjDif-Pdif	1.0154	10.1	10.2
SDR-PDR	1.0032	0.026	0.042
SSWCE-PSWCE	1.026	-3.7	13.2
SCldTr-PCldTr	0.978	0.0106	0.033
SScv-PScv	0.9911	0.0092	0.062

but with a significant offset of 2.6% and a standard deviation of over 4%. For the three SW Flux Analysis derived variables included in the study, the slopes are near unity with relatively small offsets and standard deviations, except for the previously noted standard deviation of the sky cover comparison.

Summary:

The prototype SPN-1 radiometer was tested by comparison over a roughly six month period with collocated PARSL tracker-mounted radiometers. The results show a multiplicative bias for the total SW that suggests a calibration factor error that can easily be accounted for using an empirically derived adjustment factor which on average eliminates the bias. Naturally, due to the instrument detector and shading pattern design, comparisons of the total SW using short time averages exhibit scatter in the comparisons amounting to a standard deviation of about 14 Wm^{-2}.

The SPN-1 diffuse SW, even after the same adjustment factor used for the total SW is applied, still exhibits a significant underestimation compared to PARSL diffuse SW measurements. This low bias at times produces sub-Rayleigh diffuse measurements even for the adjusted values. Additionally, the SPN-1 diffuse SW time series exhibits anomalous variations under clear skies that do not represent any physical phenomenon associated with the skylight itself. It is speculated that the cause of these two anomalous behaviors might have roots in the internal heating design of the SPN-1, and a corresponding effect on the heat transfer of the thermopiles. These two concerns negatively impact the SPN-1 diffuse SW data, significantly increasing the uncertainty of these measurements especially under clear skies. The diffuse SW underestimation exhibits no fractional sky cover dependence, which also suggests this is not caused by spectral response issues, but does suggest it may be possible to apply an additional adjustment for the diffuse to decrease the underestimation in the mean. However the anomalous time variability still presents a problem with regard to the accuracy of the diffuse SW measurements, especially on shorter time scales.

Nevertheless, the SPN-1 data as is have been shown to be adequate for detecting clear skies and estimating SW cloud effects, cloud transmissivity, and fractional sky cover using the Flux Analysis methodology. This represents a significant achievement given a relatively inexpensive instrument with no moving parts. For those situations where deployment of a solar tracker and multi-instrument systems is not practical (remote deployments, power limitations, minimization of moving parts for marine deployments, etc.), then the SPN-1 deployed along with a standard unshaded pyranometer is certainly a viable alternative to gather the data necessary for application of the Flux Analysis methodology. If the anomalous diffuse SW low bias and variability issues can be addressed, perhaps the SPN-1 instrument alone (without a collocated standard unshaded pyranometer) might be a viable solution for remote deployments.

References:

Dutton, E. G., J. J. Michalsky, T. Stoffel, B. W. Forgan, J. Hickey, D. W. Nelson, T. L. Alberta, and I. Reda, (2000). Measurement of broadband diffuse solar irradiance using current commercial instrumentation with a correction for thermal offset errors. J. Atmos. and Ocean. Tech., 18(3), 297-314.

Long, C. N. and T. P. Ackerman, (2000): Identification of Clear Skies from Broadband Pyranometer Measurements and Calculation of Downwelling Shortwave Cloud Effects, JGR, 105, No. D12, 15609-15626.

Long, C. N. and E. G. Dutton, (2002): BSRN Global Network recommended QC tests, V2.0, BSRN Technical Report, available via (http://ezksun3.ethz.ch/bsrn/admin/dokus/qualitycheck.pdf)

Long, C. N. and K. L. Gaustad, (2004): The Shortwave (SW) Clear-Sky Detection and Fitting Algorithm: Algorithm Operational Details and Explanations, Atmospheric Radiation Measurement Program Technical Report, ARM TR-004, 26 pp., Available via http://www.arm.gov/publications/techreports.stm.

Long, C. N. and Y. Shi, (2006): The QCRad Value Added Product: Surface Radiation Measurement Quality Control Testing, Including Climatologically Configurable Limits, Atmospheric Radiation Measurement Program Technical Report, ARM TR-074, 69 pp., Available via http://www.arm.gov/publications/techreports.stm.

Long, C. N., T. P. Ackerman, K. L. Gaustad, and J. N. S. Cole, (2006): Estimation of fractional sky cover from broadband shortwave radiometer measurements, JGR, 111, D11204, doi:10.1029/2005JD006475.

Press, W. H., B. P. Flannery, S. A. Teukolsky, and W. T. Vetterling (1986), Numerical recipes: The art of scientific computing, 818 pp., Cambridge Univ. Press, New York.

Younkin, K. and C. N. Long, (2004): Improved Correction of IR Loss in Diffuse Shortwave Measurements: An ARM Value Added Product, Atmospheric Radiation Measurement Program Technical Report, ARM TR-009, 50 pp., Available via http://www.arm.gov/publications/techreports.stm.

Pacific Northwest
NATIONAL LABORATORY

Proudly Operated by **Battelle** *Since 1965*

U.S. DEPARTMENT OF
ENERGY

902 Battelle Boulevard
P.O. Box 999
Richland, WA 99352
1-888-375-PNNL (7665)

www.pnnl.gov